Mol Neurobiol (2016) 53:968–982
DOI 10.1007/s12035-014-9061-6

Cypermethrin Stimulates GSK3β-Dependent Aβ and p-tau Proteins and Cognitive Loss in Young Rats: Reduced HB-EGF Signaling and Downstream Neuroinflammation as Critical Regulators

Shailendra Kumar Maurya · Juhi Mishra · Sabiya Abbas · Sanghamitra Bandyopadhyay

Received: 16 September 2014 / Accepted: 9 December 2014 / Published online: 10 January 2015

Abstract Pesticide exposure is recognized as a risk factor for Alzheimer's disease (AD). We investigated early signs of AD-like pathology upon exposure to a pyrethroid pesticide, cypermethrin, reported to impair neurodevelopment. We treated weanling rats with cypermethrin (10 and 25 mg/kg) and detected dose-dependent increase in the key proteins of AD, amyloid beta (Aβ), and phospho-tau, in frontal cortex and hippocampus as early as postnatal day 45. Upregulation of Aβ pathway involved an increase in amyloid precursor protein (APP) and its pro-amyloidogenic processing through beta-secretase (BACE) and gamma-secretase. Tau pathway entailed elevation in tau and glycogen-synthase kinase-3-beta (GSK3β)-dependent, phospho-tau. GSK3β emerged as a molecular link between the two pathways, evident from reduction in phospho-tau as well as BACE upon treating GSK3β inhibitor, lithium chloride. Exploring the mechanism revealed an attenuated heparin-binding epidermal growth factor (HB-EGF) signaling and downstream astrogliosis-mediated neuroinflammation to be responsible for inducing Aβ and phospho-tau. Cypermethrin caused a proximal reduction in HB-EGF, which promoted astrocytic nuclear factor kappa B signaling and astroglial activation close to Aβ and phospho-tau. Glial activation stimulated generation of interleukin-1 (IL-1), which upregulated GSK3β, and APP and tau as well, resulting in co-localization of Aβ and phospho-tau with IL-1 receptor. Intracerebral insertion of exogenous HB-EGF restored its own signaling and suppressed neuroinflammation and thereby Aβ and phospho-tau in cypermethrin-exposed rats, proving a central role of reduced HB-EGF signaling in cypermethrin-mediated neurodegeneration. Furthermore, cypermethrin stimulated cognitive impairments, which could be prevented by exogenous HB-EGF. Our data demonstrate that cypermethrin induces premature upregulation of GSK3β-dependent Aβ and tau pathways, where HB-EGF signaling and neuroinflammation serve as essential regulators.

Keywords Pyrethroid · Growth factor · NF-κB · Astrogliosis · Neurodegeneration

Introduction

Alzheimer's disease (AD) is one of the most common forms of neurodegenerative disorders [1], and populations residing in regions with high pesticide usage have an increased likelihood of developing the disease, independent of age [2]. Cypermethrin is a widely used pyrethroid pesticide for agricultural and household purposes, reported to be toxic to the developing brain [3]. Early-life exposure to cypermethrin induces neuronal cell dysfunctions [3, 4] that affects synaptic activity and evokes neurodegeneration [5]. Although a human population-based study suggests pyrethroid pesticide exposure as a risk for AD [2], the mechanisms are un-elucidated. Here, we studied the effects of early-life exposure to cypermethrin on markers of AD in the young rat brain.

Electronic supplementary material The online version of this article (doi:10.1007/s12035-014-9061-6) contains supplementary material, which is available to authorized users.

S. K. Maurya · J. Mishra · S. Bandyopadhyay (✉)
Developmental Toxicology, Council of Scientific and Industrial Research-Indian Institute of Toxicology Research (CSIR-IITR), Lucknow 226001, India
e-mail: sanghmitra@iitr.res.in

S. Abbas
Food and Chemical Toxicology, Council of Scientific and Industrial Research-Indian Institute of Toxicology Research (CSIR-IITR), Lucknow 226001, India

Elevation in amyloid beta (Aβ) and microtubule-associated phospho (p)-tau protein in frontal cortex and hippocampus are the key characteristics of AD [6, 7]. This leads to disruption in neuronal activity that engenders a decline in cognitive performances [8–10]. The amyloid hypothesis postulates a proteolytic cleavage of amyloid precursor protein (APP) by beta-secretase (BACE) to release C-terminal fragment (CTF-β) that is then cleaved by gamma (γ)-secretase to generate $A\beta_{1-42}$ and less amyloidogenic, $A\beta_{1-40}$ [11]. Tau pathology entails an accumulation of tau protein and its abnormally phosphorylated form [12]. A constitutively active, proline-directed serine/threonine kinase, glycogen synthase kinase-3β (GSK3β), is the chief inducer of p-tau [13]. GSK3β is reported to regulate the APP amyloidogenic processing as well, through modulation of γ-secretase functioning [14, 15]. A study also claims regulation of BACE expression by GSK3β, inducing modulation in AD-associated phenotypes [16]. Here, we explored the effects of cypermethrin on APP amyloidogenic and tau pathways. We further examined whether GSK3β regulated the two pathways.

Neuroinflammation, via the nuclear factor kappa B (NF-κB) signaling, plays an important role in the etiology of AD [17, 18]. Activated astrocyte and microglial cells secrete pro-inflammatory cytokines that accelerate an amyloid plaque buildup [19] and enhance GSK3β activity exacerbating tau pathology [20]. Cypermethrin is reported to promote the generation of IL-1 in the striatum of an adult brain [21]; however, whether cypermethrin stimulates cortical and hippocampal neuroinflammation, and its' relation to AD-like pathology is unknown.

We reported that cypermethrin induces apoptosis in astrocytes through blocking of heparin-binding epidermal growth factor (HB-EGF)-epidermal growth factor receptor (EGFR) signaling [22]. HB-EGF functions as an endogenous neuroprotective agent [23] that regulates memory and cognitive performance [24, 25]. HB-EGF signaling is also described to affect progression of neuroinflammatory disorders [26, 27]. However, whether an alteration in HB-EGF signaling regulates inflammation mediated AD pathogenesis remains unidentified.

Here, we explored induction of Aβ and p-tau proteins, as well as GSK3β in frontal cortex and hippocampus of cypermethrin-exposed young rats. We examined the association of HB-EGF, NF-κB signaling, and neuroinflammation with Aβ and p-tau. Overall, the importance of this study is twofold, as it provides a molecular mechanism governing cypermethrin-mediated early manifestations of AD-like pathology, and points to a novel role of HB-EGF in regulating Aβ and p-tau induction.

Materials and Methods

Reagents and Antibodies

Cypermethrin, Ponceau S stain, Hoechst 33258, lithium chloride (LiCl), and reagents for Western blotting were from Sigma Chemical Co. (St. Louis, MO). Sample loading buffer and protein ladder for Western blotting were from Invitrogen (Carlsbad, CA). Mouse monoclonal β-actin (catalog (cat.) no. A5441), rabbit monoclonal glial fibrillary acidic protein (GFAP; cat. no. G9269), rabbit polyclonal $A\beta_{1-42}$ (for enzyme-linked immunosorbent assay (ELISA); cat. no. A1976), rabbit polyclonal C-terminal fragment (CTFβ; cat. no. A8717) antibodies, horseradishperoxide (HRP)-conjugated secondary antibodies, anti-rabbit IgG (cat. no. A0545), antimouse IgG (cat. no. A9044), and antigoat IgG (cat. no. A5420) were from Sigma Chemical Co. Rabbit polyclonal microtubule-associated protein 2 (MAP2; cat. no.4542S)) (for co-immunolabeling with p-tau), rabbit monoclonal PS1(cat. no. 5643S), rabbit polyclonal PS2 (cat. no. 2192S), rabbit polyclonal EGFR (cat. no. 2232S), rabbit monoclonal phospho (p)-EGFR (cat. no. 3777S), rabbit monoclonal GSK3β (cat. no. 9315BC), mouse monoclonal phospho-I-kappa (p-IκB; cat. no. 2859), mouse monoclonal p-tau (Ser396) (cat. no. 9632BC), and tau (cat. no.4019S) antibodies were from Cell Signaling Technology (Danvers, MA). Goat polyclonal HB-EGF (cat. no. sc-1414) antibody, mouse monoclonal p65-NF-κB (sc-8008) and rabbit polyclonal interleukin-1 receptor type 1 (IL-1R1; cat. no. sc-689) antibody were obtained from Santa Cruz Biotechnology (Dallas, TX). Rabbit polyclonal IL-1α (cat. no. ab7632), rabbit polyclonal IL-1β (cat. no. ab2105), rabbit polyclonal APP (cat. no. ab15272), rabbit polyclonal $A\beta_{1-42}$ (cat. no. ab10148), mouse monoclonal Iba1 (cat. no. ab15690) and rabbit polyclonal CD68 (cat. no. ab125047) antibodies, and BACE activity kit (cat. no. ab65357) were from Abcam (Cambridge, MA). Mouse monoclonal GFAP (cat. no. MAB360) and mouse monoclonal $A\beta_{1-40}$ (cat. no. MAB8768) was obtained from Millipore (Temecula, CA). Super Signal West Femto Maximum Sensitivity Substrate was from Pierce Biotechnology (Rockford, IL). Recombinant human HB-EGF (259-HE) and recombinant rat IL-1 receptor antagonist (IL-1Ra cat. no. 1545-RA) were from R&D Systems (Minneapolis, MN, USA). $A\beta_{1-40}$ ELISA kit (cat. no. 27415) was from Immuno-Biological Laboratories (Gunma, Japan). Li-COR Odyssey blocking buffer, IRDye 800CW goat anti-mouse, and IRDye 680CW goat anti-rabbit secondary antibodies were from LI-COR (Lincoln, NE). Alexa Fluor® 594 goat anti-chicken, Alexa Fluor® 488 goat anti-mouse (cat. no. A11003), and Alexa Fluor® 568 goat anti-rabbit (cat. no. A11010) secondary antibodies were from Invitrogen. Chicken polyclonal MAP2 (cat. no. 014460) antibody

was from Stem Cell Technologies Inc. (West Seventh Avenue, Canada).

Animals and Treatments

The overall treatment timeline is as shown in Suppl. 1.

Regulations of the Institutional Animal Ethical Committee (CSIR-IITR) were followed for animal handling. Twenty-four-day-old (postnatal-24) male Wistar rats were housed in a 12-h day and light cycle environment with the ad libitum availability of diet and water (R. O.). The postnatal-24 rats were daily gavage-treated with equal volumes of vehicle (corn oil) or cypermethrin (dissolved in corn oil) at doses of 10 or 25 mg/kg, i.e., 1/25 and 1/10 of lethal dose 50 (LD-50), respectively [22, 28], for 2, 3, or 6 weeks (the LD-50 value is as reported in "Reregistration ability decision for cypermethrin," EPA OPP-2005-0293, June 14 2006 (revised 1/14/2008)). To eliminate complicating consequences of the female reproductive cycle, we selected only male rats for our study.

To inhibit GSK3β, 24-day-old rats were daily gavage-treated with 300 mg/kg of LiCl for 3 weeks, as previously described [29, 30]. As expected, LiCl attenuated the GSK3β levels (Suppl. 2A).

To understand the effect of exogenous HB-EGF on HB-EGF signaling in cypermethrin-treated rats, recombinant HB-EGF (100 ng in 2 μL phosphate-buffered saline (PBS)) was injected through intracerebroventricular (i.c.v.) route once in postnatal-24 rats (the HB-EGF dose was decided after standardization using 50, 100, and 200 ng treatment doses, where 100 ng showed significant upregulation in cortical and hippocampal HB-EGF without inducing toxicity). Briefly, rats were anesthetized using chloral hydrate (300 mg/kg) and placed in stereotaxic frames (Stoelting Co., USA), skull exposed, and disinfected with betadine. An incision was made in the scalp, drilled and i.c.v. injection with recombinant HB-EGF at a slow rate (1 μL/min) was performed using 10-μL Hamilton syringe. The syringe was held in place for 5 min. The vehicle control rats were treated with sterile PBS that followed the same procedure.

To understand the effect of IL-1 on GSK3β, Aβ, and p-tau in cypermethrin-treated rats, we injected IL-1Ra (350 ng in 5 μL PBS) [31] through i.c.v. route as described above for HB-EGF injection. As expected, IL-1Ra attenuated the IL-1R1 levels (Suppl. 2B).

Protein Extraction and Western Blotting

Tissues of rat cerebral cortex and hippocampus were harvested and homogenized in tissue lysis buffer. Homogenates were centrifuged (30 min, 15,000 rpm, 4 °C) and protein concentration in lysate determined using NanoDrop™ Spectrophotometer (Thermo Scientific, Wilmington, DE). SDS-PAGE and Western blotting of lysates were then performed as described previously [32]. Blots were probed with 1:1000 dilutions (in PBS plus 0.2 % Tween 20 (PBST)) of $A\beta_{1-42}$, APP, CTFβ, PS1, PS2, GSK3β, tau, p-tau, HB-EGF, EGFR, p-EGFR, IL-1α, IL-1β, IL-1R1, GFAP, or β-actin primary antibodies, and 1:20,000 dilution of secondary antibodies conjugated to IRDye. Protein was visualized using Odyssey® CLx Infrared Imaging System (LI-COR). For HB-EGF, the secondary antibody was HRP-conjugated (1:2000 dilution) and was visualized through chemiluminescence using Supersignal West Femto Maximum Sensitivity Substrate. Protein expression was quantified using VersaDoc Gel Imaging System (BioRad, Hercules, CA).

Immunofluorescence

Briefly, rats were anesthetized, perfused with 4 % p-formaldehyde (PFA) in PBS, and whole brain dissected [33]. The brain was post-fixed in PFA, cryoprotected in 30 % sucrose, and cryosectioned (5 μm) using cryomicrotome (Microm HM 520; Labcon, Munich, Germany). The sections were mounted on 3-aminopropyltriethoxysilane-coated slides, antigen-retrieved, and blocked with 3 % donkey serum in PBS. Sections were then probed with 1:200 dilution of $A\beta_{1-42}$, p-tau, MAP2, Iba-1, CD68, p-IκBα, NF-κB, or IL-1R1 antibody, and 1:400 dilution of GFAP primary antibody. Sections were then treated with Alexa Fluor secondary antibodies at 1:400 dilution compared to respective primary antibodies, counterstained with Hoechst 33258 (0.2 mM), mounted in Vectashield media and visualized under a fluorescence microscope (Nikon Instech Co. Ltd., Kawasaki, Kanagawa, Japan) using ×10 and ×40 objectives. Images were captured using Image-Pro Plus 5.1 software (Media Cybernetics Inc., Silver Spring, MD), and imported into ImageJ 1.42q (http://rsb.info.nih.gov/ij/; Wayne Rasband, National Institutes of Health, Bethesda, MD) for image analysis.

$A\beta_{1-40}$ and $A\beta_{1-42}$ ELISA

$A\beta_{1-40}$ levels were determined using its ELISA kit. Briefly, tissue was homogenized in extraction buffer and centrifuged (45 min, 40,000 rpm, 4 °C). The supernatant was added to $A\beta_{1-40}$-precoated plates, incubated overnight (4 °C), and treated with wash buffer. The plates were then incubated with labeled antibody in dark (1 h, 4 °C), washed, incubated with chromogen (30 min) and treated with stop solution. Sample absorbance was read at 450 nm using FLUOstar Omega multimode microplate reader (BMG LABTECH, Ortenberg, Germany). $A\beta_{1-40}$ concentration (pg/mL) was calculated by comparing with standards provided with kit.

For $A\beta_{1-42}$, the protocol [34] was quite similar, except that the plates were coated with capture antibody (2–10 μg/mL) in

coating buffer. The samples were added to the plates, incubated with primary $A\beta_{1-42}$ and then with secondary HRP-conjugated antibodies with intermediate washes. The plates were then incubated with 3′,5,5′-tetramethylbenzidine substrate, followed by the addition of stop solution. Sample absorbance was read at 450 nm, and $A\beta_{1-42}$ concentration was calculated by comparing with standards of rat recombinant $A\beta_{1-42}$ peptide (Tocris Bioscience, Bristol, UK).

BACE Assay

BACE activity was determined using its assay kit. Briefly, tissue was homogenized in extraction buffer and centrifuged (30 min, 14,000 rpm, 4 °C). The supernatant was added to 96-well dark plates, treated with secretase reaction buffer and BACE substrate, and incubated for 1 h at 37 °C. Sample fluorescence was read at excitation 335–355 nm and emission 495–510 nm using microplate reader. BACE activity (relative fluorescence unit) was calculated by comparing with standards provided with kit.

Learning Memory Test by Y-Maze

The Y-Maze apparatus had an illuminated safe arm without foot shock, while the other arms were dark and with electric foot shock (1–5 mA). Rats were first trained for 30 trials during learning to discriminate safe and unsafe area, and running into unsafe area was counted as an error (E) [33]. During the test, the memory retention for discriminating safe and unsafe area at 24 h, 48 h, and 7 days post-learning was determined and is expressed as follows: % saving memory$=(E_{\text{training}}-E_{\text{test}})\times 100/E_{\text{training}}$.

Learning Memory Test by Passive Avoidance Test

Rats were placed in illuminated compartment of a shuttle box (Techno, India), separated from the dark compartment by a sliding door. After 30-s acclimatization, rats were allowed to enter the dark compartment where it received a low intensity foot shock (0.5 mA) for 10 s (acquisition (aq)). During retention (R), rats were made to undergo successive trials at 24 h (R1), 48 h (R2), and 72 h (R3) post-acquisition, and time taken by rats to move from light to dark compartment was counted as transfer latency time [35].

Statistical Analysis

Data are presented as means±SE. Statistical analysis was performed using GraphPad Prism software (GraphPad Software, Inc., La Jolla, USA), and the data were analyzed using one-way ANOVA, followed by Bonferroni's test.

Results

Effect of Cypermethrin on Aβ and p-tau Levels in Young Rats

We orally fed 24-day-old rats with cypermethrin at 10 and 25 mg/kg doses (reported by us to impair neurodevelopment [22]), and checked for the two major protein indicators of AD, viz., $A\beta_{1-42}$ and p-tau, in frontal cortex and hippocampus. We observed a dose- and time-dependent increase in $A\beta_{1-42}$ (Fig. 1a) and p-tau (Fig. 1b). Exposure up to 2 weeks showed a less significant change, and 3 and 6 weeks demonstrated a strongly significant effect on $A\beta_{1-42}$ and p-tau levels (Fig. 1a, b). Therefore, we continued our study up to 3 weeks, i.e., the earliest time point demonstrating a prominent effect. Through co-immunostaining with neuronal microtubule-associated protein, MAP2, we verified enhanced neuronal expression of $A\beta_{1-42}$ (Fig. 1c) and p-tau (Fig. 1d) in frontal cortex and hippocampus at 3-week exposure.

We then examined the effect of cypermethrin on the less amyloidogenic, $A\beta_{1-40}$ peptide. Consistent with $A\beta_{1-42}$ data, we observed a dose-dependent increase in $A\beta_{1-40}$ (Fig. 1e). We assessed the $A\beta_{1-42}/A\beta_{1-40}$ ratio that plays a critical role in AD [36]. For this, we performed ELISA for $A\beta_{1-42}$ and $A\beta_{1-40}$, and calculated the ratio. ELISA data corroborated the Western blot data, showing dose-dependent increase in both the Aβ isoforms (Fig. 1f), and their ratio (calculated from the ELISA data) was >1.0 (Fig. 1g), indicating elevated amyloidogenicity.

Effect of Cypermethrin on APP Cleavage and tau Phosphorylation Pathways

We studied whether cypermethrin affected the amyloidogenic pathway of APP processing. For this, we first looked into the expression levels of APP and measured BACE activity and expression levels of γ-secretase components, PS1 and PS2. We detected a cypermethrin-mediated increase in APP (Fig. 2a), BACE enzymatic activity (Fig. 2b), and PS1 and PS2 (Fig. 2c). We then assessed the tau phosphorylation pathway, and found an increase in tau (Fig. 2d), as well as the major tau kinase, GSK3β (Fig. 2e).

To identify any possible link between APP cleavage and tau phosphorylation pathways, we focused upon GSK3β, reported to facilitate Aβ production, besides inducing p-tau [14–16]. We found that the GSK3β inhibitor, LiCl, prevented cypermethrin-mediated induction of Aβ (Fig. 2f), besides p-tau (Fig. 2g). We further screened, using LiCL, for the specific molecule of the amyloidogenic pathway targeted by GSK3β. We observed a LiCl-mediated reduction in BACE (Fig. 2h), revealing GSK3β-dependent induction of BACE upon

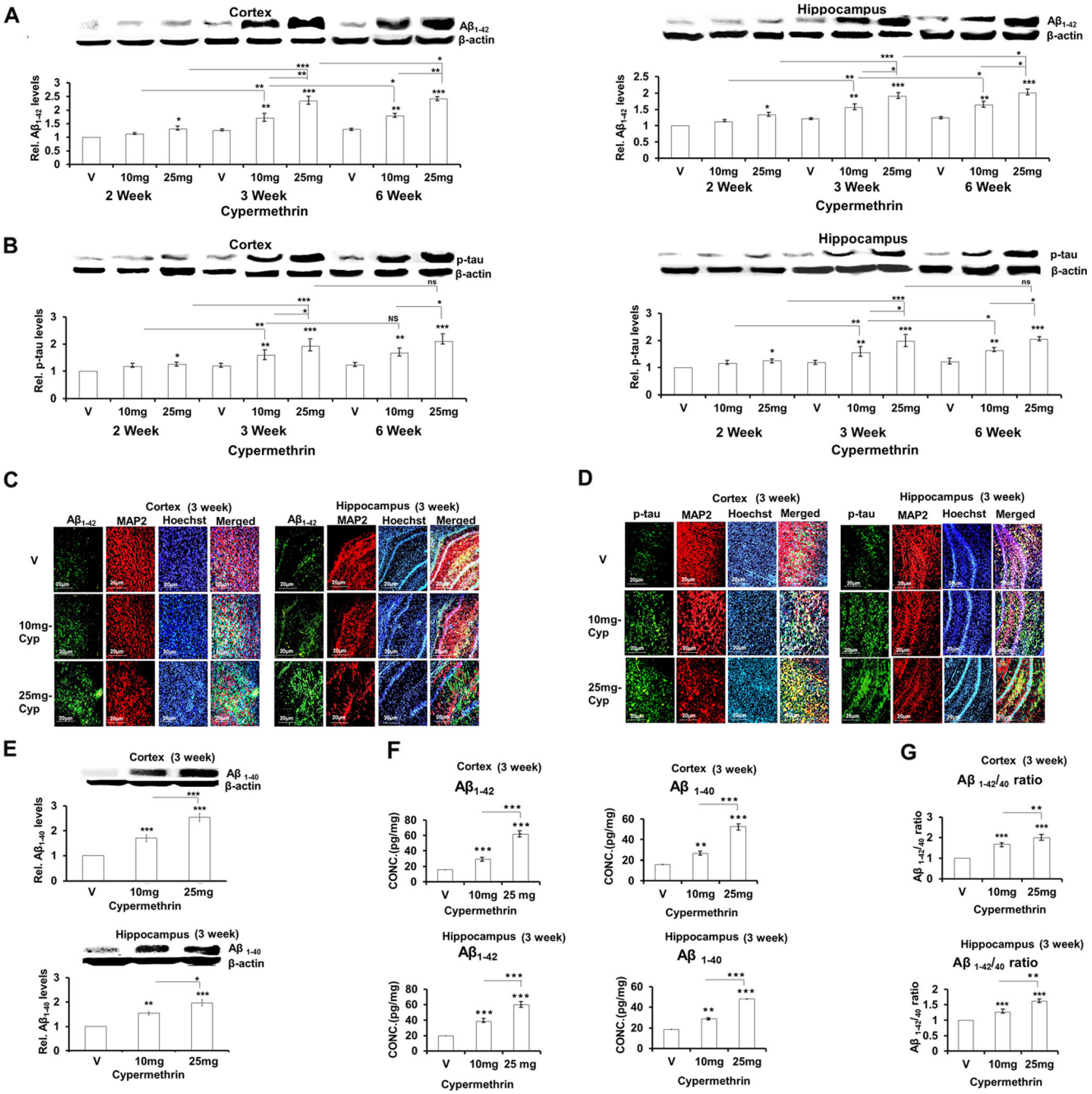

Fig. 1 Cypermethrin upregulates Aβ and p-tau in young rat frontal cortex and hippocampus. Representative Western blot and densitometry showing dose- and time-dependent increase in $A\beta_{1–42}$ (15 kDa) (**a**) and p-tau (50 kDa) (**b**) normalized with β-actin (42 kDa) in cortex (LHS) and hippocampus (RHS). Representative photomicrograph (×10 magnification) of $A\beta_{1–42}$ (**c**) (*green fluorescence*) or p-tau (**d**) (*green fluorescence*), MAP2 (*red fluorescence*), nucleus (*blue fluorescence*), and the three merged in the same field in cortex (*left panel*) and hippocampus (*right panel*). **e** Representative Western blot and densitometry showing a dose-dependent increase in $A\beta_{1–40}$ (25 kDa) normalized with β-actin in cortex (*upper panel*) and hippocampus (*lower panel*). **f** Dose-dependent increase in $A\beta_{1–42}$ (LHS) and $A\beta_{1–40}$ (RHS) in cortex (*upper panel*) and hippocampus (*lower panel*), determined through ELISA. **g** Increase in $A\beta_{1–42}/A\beta_{1–40}$ ratio in cortex (*upper panel*) and hippocampus (*lower panel*). Western blot data represent means±SE of five rats. ***$P<0.001$, **$P<0.01$, and *$P<0.05$ compared to vehicle (V) or as indicated; *ns* non-significant. The sections for immunofluorescence are representatives of five different rats

cypermethrin exposure. We verified this by checking the levels of BACE-derived cleavage product, CTFβ [11]. We observed a reduction in cypermethrin-induced CTFβ upon LiCl treatment (Fig. 2i).

Thus, cypermethrin stimulated GSK3β, which increased p-tau expression and upregulated BACE activity. Therefore, GSK3β served as the molecular link between cypermethrin-induced neuronal p-tau and Aβ.

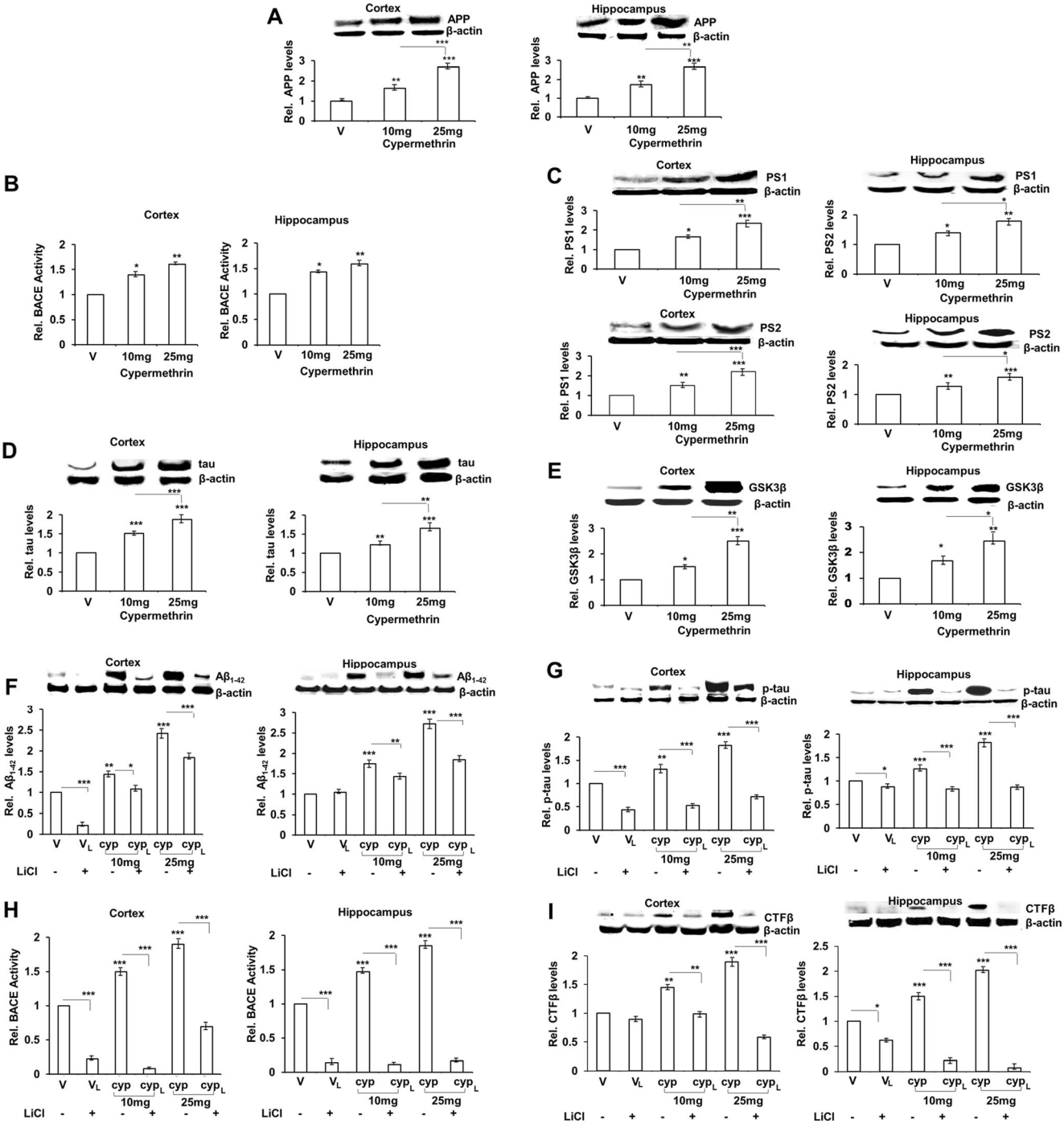

Fig. 2 Cypermethrin upregulates APP amyloidogenic processing and tau phosphorylation. **a** Representative Western blot and densitometry showing dose-dependent increase in APP (87 kDa) normalized with β-actin in cortex (LHS) and hippocampus (RHS). **b** Relative increase in BACE activity in cortex (LHS) and hippocampus (RHS). **c** Representative Western blot and densitometry showing dose-dependent increase in PS1 (22 kDa, *upper panel*) and PS2 (23 kDa, *lower panel*) in cortex (LHS) and hippocampus (RHS). Representative western blot and densitometry showing dose-dependent increase in tau (50 kDa) (**d**) and GSK3β (46 kDa) (**e**) normalized with β-actin in cortex (LHS) and hippocampus (RHS). Representative Western blot and densitometry of $A\beta_{1-42}$ (**f**) and p-tau (**g**) normalized with β-actin in cortex (LHS) and hippocampus (RHS) of rats treated with cypermethrin and/or LiCl (V= vehicle treated, V_L=LiCl+vehicle treated, Cyp=cypermethrin treated, and Cyp_L=LiCl+cypermethrin treated). **h** Relative BACE activity in cortex (LHS) and hippocampus (RHS) of rats treated with cypermethrin and/or LiCl. **i** Representative Western blot and densitometry of CTFβ normalized with β-actin in cortex (LHS) and hippocampus (RHS) of rats treated with cypermethrin and/or LiCl. Data represent means±SE of five rats. ***$P<0.001$, **$P<0.01$, and *$P<0.05$ compared to vehicle (V) or as indicated

Effect of Cypermethrin on HB-EGF Signaling, and Regulation of Aβ and p-tau by HB-EGF

We next assessed the mechanism stimulating GSK3β-mediated Aβ and p-tau induction upon cypermethrin exposure. We had earlier reported that cypermethrin reduced the levels of HB-EGF, EGFR, and p-EGFR in the rat astrocyes [22]. Here, we investigated whether cypermethrin affected the HB-EGF-EGFR signaling in rat frontal cortical and hippocampal tissues. We observed that cypermethrin caused dose-dependent reduction in HB-EGF levels in the tissues, which could be restored by treating exogenous HB-EGF (through intracerebral insertion of recombinant HB-EGF) (Fig. 3a), verifying self-regulated

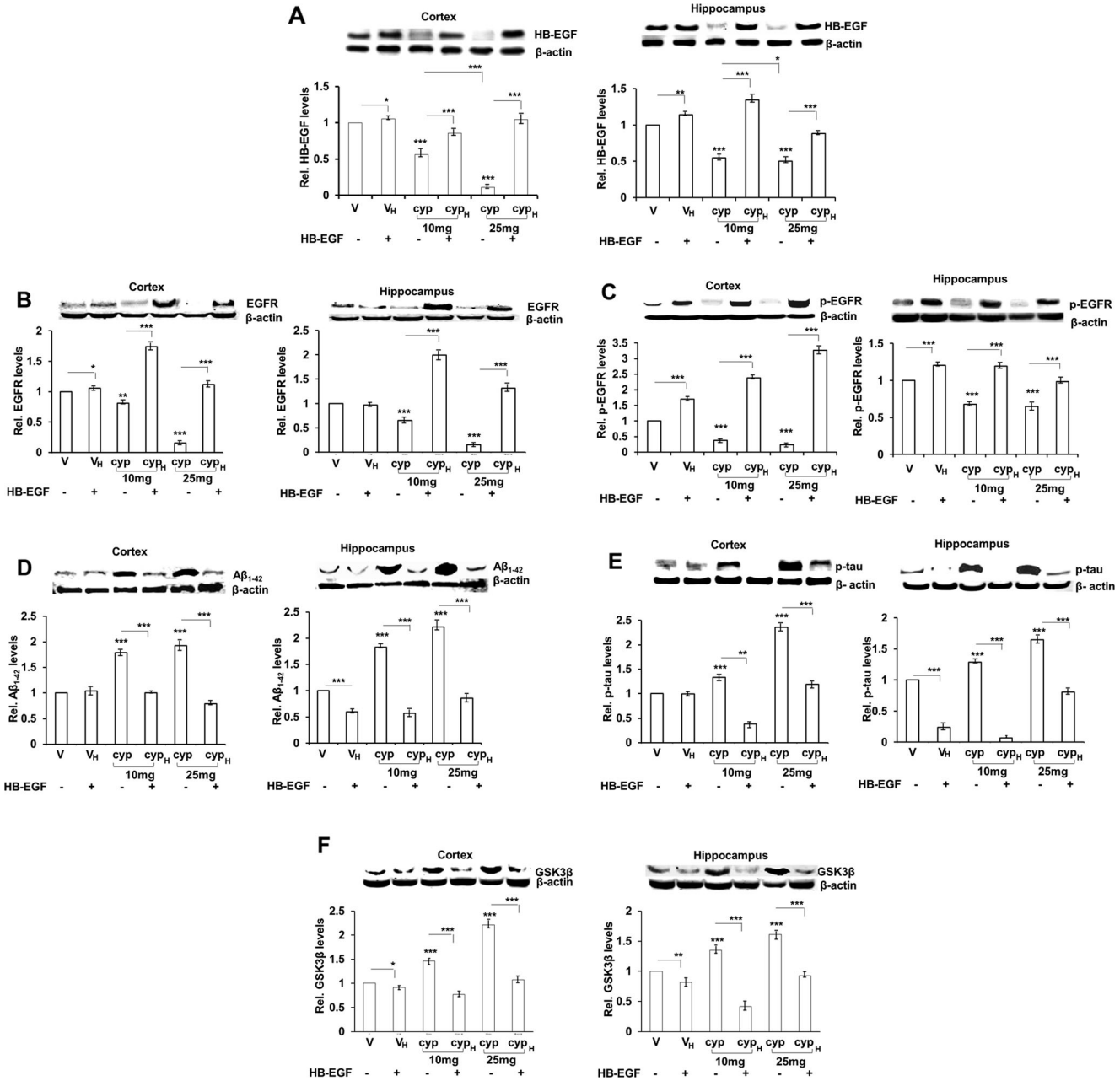

Fig. 3 Cypermethrin reduces HB-EGF signaling, which induces Aβ and p-tau induction. Representative Western blot and densitometry of HB-EGF (22 kDa) (**a**), EGFR (170 kDa) (**b**), and p-EGFR (175 kDa) (**c**) normalized with β-actin in cortex (LHS) and hippocampus (RHS) of rats treated with cypermethrin and/or HB-EGF (V=vehicle treated, V_H=HB-EGF+vehicle treated, Cyp=cypermethrin treated, and Cyp_H=HB-EGF+cypermethrin treated). Representative Western blot and densitometry of $Aβ_{1–42}$ (**d**), p-tau (**e**), and GSK3β (**f**) normalized with β-actin in cortex (LHS) and hippocampus (RHS) of rats treated with cypermethrin and/or HB-EGF. Data represent means±SE of five rats. ***$P<0.001$, **$P<0.01$, and *$P<0.05$ compared to vehicle (V) or as indicated

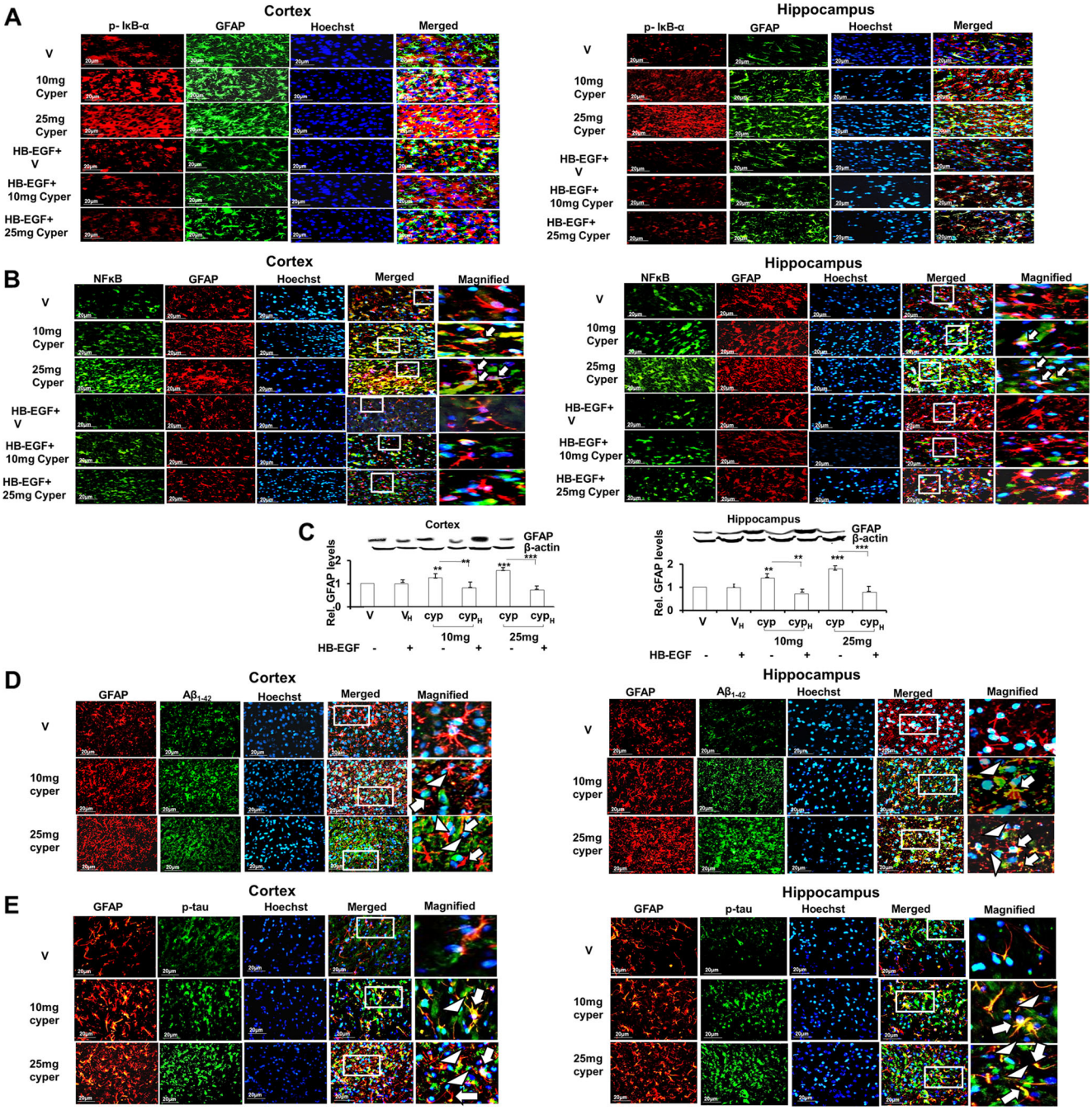

Fig. 4 Cypermethrin promotes NF-κB signaling and induces astrogliosis. **a** Representative photomicrograph (×40 magnification) of p-IκBα (*red fluorescence*), GFAP (*green fluorescence*), nucleus (*blue fluorescence*), and the three merged in the same field in cortex (LHS) and hippocampus (RHS) of rats treated with cypermethrin and/or HB-EGF. **b** Representative photomicrograph (×40 magnification) of NF-κB (*green fluorescence*), GFAP (*red fluorescence*), nucleus (*blue fluorescence*), and the three merged in the same field in cortex (LHS) and hippocampus (RHS). *Magnified image* shows magnification of the inset area from *merged image*, where the *arrow* indicates nuclear localization. **c** Representative Western blot and densitometry of GFAP (52 kDa) normalized with β-actin in rats treated with cypermethrin and/or HB-EGF (V=vehicle treated, V_H=HB-EGF+vehicle treated, Cyp=cypermethrin treated, and Cyp_H=HB-EGF+cypermethrin treated). Representative photomicrograph (×40 magnification) of GFAP (*red fluorescence*), $A\beta_{1-42}$ (*green fluorescence*) (**d**) or p-tau (*green fluorescence*) (**e**), nucleus (*blue fluorescence*), and the three merged in the same field. *Magnified image* shows magnification of the inset area from *merged image*, where the *arrow* and *arrowhead* indicate GFAP and $A\beta_{1-42}$ or p-tau, respectively. Western blot data represent means±SE of five rats. ***$P<0.001$ and **$P<0.01$ compared to vehicle (V) or as indicated. The sections for immunofluorescence are representatives of five different rats

HB-EGF expression in the rat brain. Extrapolating our previous in vitro observations [22], cypermethrin suppressed tissue levels of EGFR (Fig. 3b) and p-EGFR (Fig. 3c) which could be restored by the

exogenous HB-EGF, confirming an HB-EGF-dependent EGFR signaling in the rat brain.

We next determined whether the disrupted HB-EGF signaling correlated with Aβ and p-tau induction. Treatment with exogenous HB-EGF caused a reduction in cypermethrin-induced $A\beta_{1–42}$ (Fig. 3d) and p-tau (Fig. 3e), suggesting an inverse dependence of $A\beta_{1–42}$ and p-tau on HB-EGF levels. We examined whether the disrupted HB-EGF signaling affected GSK3β. We found that the exogenous HB-EGF inhibited cypermethrin-mediated increase in GSK3β (Fig. 3f), verifying the inverse dependence of GSK3β on HB-EGF levels. Thus, cypermethrin caused a reduction in HB-EGF signaling that leads to an increase in GSK3β-mediated Aβ and p-tau induction.

Effect of Cypermethrin on NF-κB Signaling and Glial Activation

We reported that cypermethrin-mediated reduction in HB-EGF signaling evoked astrocyte apoptosis in the young rat brain [22]. Enhanced NF-κB signaling and astroglial activation associates with astrocyte atrophy in the AD brain [37, 38]. Therefore, we hypothesized an NF-κB signaling and astroglial activation to be contributing toward Aβ and p-tau induction in cypermethrin-exposed rats. We first examined NF-κB signaling and detected a cypermethrin-mediated increase in p-IκB (Fig. 4a) and NF-κB (Fig. 4b), and nuclear localization of the latter (Fig. 4b, the arrow indicating nuclear localization of NF-κB in the magnified image) in GFAP-expressing astrocytes indicating enhanced NF-κB activation in the astrocytes. To know whether increase in NF-κB signaling was related to the attenuated HB-EGF, we measured p-IκB and NF-κB in the presence of exogenous HB-EGF. Exogenous HB-EGF suppressed astrocytic p-IκB (Fig. 4a) and NF-κB (Fig. 4b) and reduced nuclear localization of the latter (Fig. 4b), suggesting an inverse dependence of astrocytic NF-κB on HB-EGF. We then checked for the astroglial activation marker, GFAP [39, 40], and found that cypermethrin promoted GFAP expression, which could also be suppressed by exogenous HB-EGF (Fig. 4c). Thus, cypermethrin reduced HB-EGF signaling, which stimulated astrocytic NF-κB signaling and astroglial activation in the rat frontal cortex and hippocampus. Because reactive astrogliosis contributes to AD [41], we assessed any association between the activated astroglial cells and Aβ and p-tau. Co-immunolabeling with GFAP and Aβ or p-tau revealed an increase in the localization of GFAP in close proximity of Aβ (Fig. 4d) and p-tau (Fig. 4e) (the arrow and arrowheads showing GFAP and Aβ or p-tau respectively), indicating astroglial activation to be associated with Aβ and p-tau.

Thus, a reduction in HB-EGF stimulates NF-κB signaling and induces astroglial activation that closely associates with increased Aβ and p-tau. Microglial activation close to $A\beta_{1–42}$ and p-tau (Suppl. 3) supported the concept of glial activation-associated AD-like pathology upon cypermethrin exposure.

Effect of Cypermethrin on Neuroinflammation

NF-κB signaling and glial activation generate inflammatory mediators that drive AD-like pathology [18]. Therefore, to verify inflammation, we checked for the expression levels of the inflammatory mediators, IL-1α and IL-1β, and their receptor IL-1R1 in the frontal cortex and hippocampus. We observed an increase in both the isoforms of IL-1 (Fig. 5a, b), as well as IL-1R1 (Fig. 5c) upon cypermethrin exposure. We then checked whether the attenuation in HB-EGF affected IL-1. We found that the exogenous HB-EGF suppressed IL-1α (Fig. 5a), IL-1β (Fig. 5b), and IL-1R1 (Fig. 5c), verifying an inverse dependence of IL-1 on HB-EGF. The inability of IL-1Ra to alter HB-EGF (data not shown) proved the attenuation of HB-EGF to be upstream of neuroinflammation.

We further verified involvement of IL-1 in Aβ and p-tau induction, by co-immunolabeling IL-1R1 with $A\beta_{1–42}$ or p-tau. We detected an increased merging of IL-1R1 with both Aβ (Fig. 5d) and p-tau (Fig. 5e). We then examined whether IL-1 was linked to GSK3β by co-treating cypermethrin-exposed rats with the exogenous IL-1 receptor antagonist, IL-1Ra (through intracerebral insertion), and measuring GSK3β levels. IL-1Ra suppressed GSK3β (Fig. 5f) and thereby $A\beta_{1–42}$ and p-tau (Suppl. 4), indicating an IL-1-mediated induction of GSK3β that led to Aβ and p-tau. We then checked whether IL-1 affected the precursor molecules of Aβ and p-tau, i.e., APP and tau. We detected that IL-1Ra suppressed APP (Fig. 5g) and tau (Fig. 5h), indicating their IL-1-dependent induction.

Thus, cypermethrin disrupts HB-EGF signaling, which promotes the generation of IL-1. IL-1 upregulates APP and tau as well as GSK3β, resulting in an increase in Aβ and p-tau in young rat frontal cortex and hippocampus.

Effect of Cypermethrin and HB-EGF on Learning-Memory Performance

Increase in Aβ and p-tau in the rat frontal cortex and hippocampus is known to affect cognitive functions [8, 10], and therefore, we investigated whether cypermethrin had any effect on rat learning-memory performances by carrying out Y-Maze and passive avoidance tests. We also examined the effect of exogenous HB-EGF on learning-memory performances in cypermethrin-exposed rats. We observed that with cypermethrin alone, the rats exhibited dose-dependent errors during training (learning), and a reduction in memory (post-learning) performance at 24 h, 48 h, and 7 days post-learning in Y-Maze test (Fig. 6a). In passive avoidance test, the rats showed a less significant increase in transfer latency time of retention trials against acquisition trials (Fig. 6b), confirming

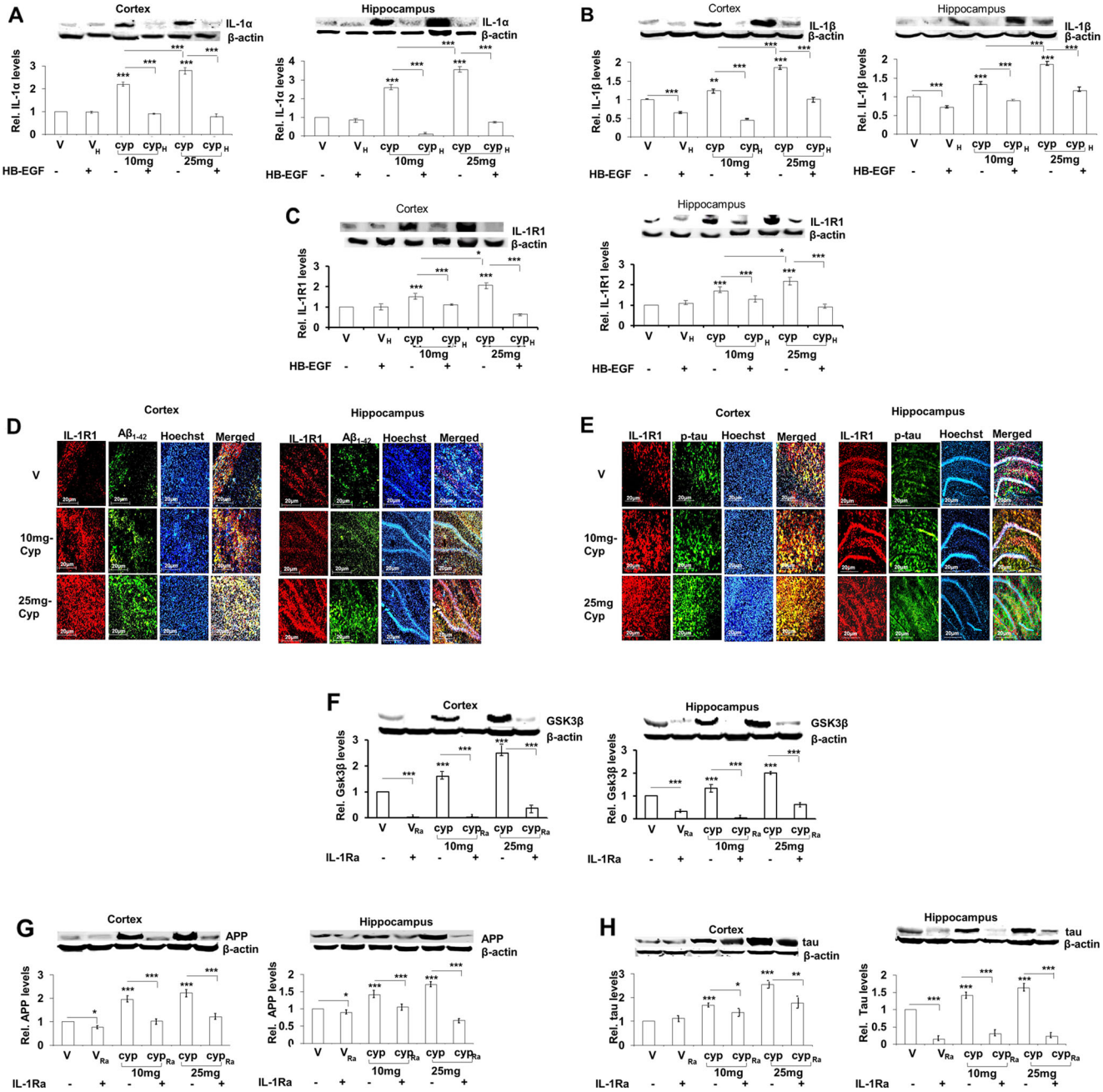

Fig. 5 Cypermethrin induces neuroinflammation. Representative Western blot and densitometry of IL-1α (17 kDa) (**a**), IL-1β (17 kDa) (**b**), and IL-1R1(80 kDa) (**c**) normalized with β-actin in cortex (LHS) and hippocampus (RHS) of rats treated with cypermethrin and/or HB-EGF (V=vehicle treated, V_H=HB-EGF+vehicle treated, Cyp=cypermethrin treated, and Cyp_H=HB-EGF+cypermethrin treated). Representative photomicrograph (×10 magnification) of IL-1R1 (*red fluorescence*), $A\beta_{1-42}$ (*green fluorescence*) (**d**) or p-tau (*green fluorescence*) (**e**), nucleus (*blue fluorescence*), and the three merged in the same field in cortex (LHS) and hippocampus (RHS). Representative Western blot and densitometry of GSK3β (**f**), APP (**g**), and tau (**h**) normalized with β-actin in cortex (LHS) and hippocampus (RHS) of rats treated with cypermethrin and/or IL-1Ra (V=vehicle treated, V_{Ra}=IL-1Ra+vehicle treated, Cyp=cypermethrin treated, and Cyp_{Ra}=IL-1Ra+cypermethrin treated). Data represent means±SE of five rats. ***$P<0.001$, **$P<0.01$, and *$P<0.05$ compared to vehicle (V) or as indicated. The sections for immunofluorescence are representatives of five different rats

reduction in learning-memory performance. Exogenous HB-EGF inhibited cypermethrin-mediated changes in learning-memory performance in Y-Maze (Fig. 6c) and passive avoidance tests (Fig. 6d), indicating an HB-EGF-dependent regulation of learning-memory performances.

Schematic Representation of the Effect of Cypermethrin on AD-Like Pathology in Young Rats

Cypermethrin suppresses HB-EGF-signaling, which activates astroglial NF-κB signaling in rat frontal cortex

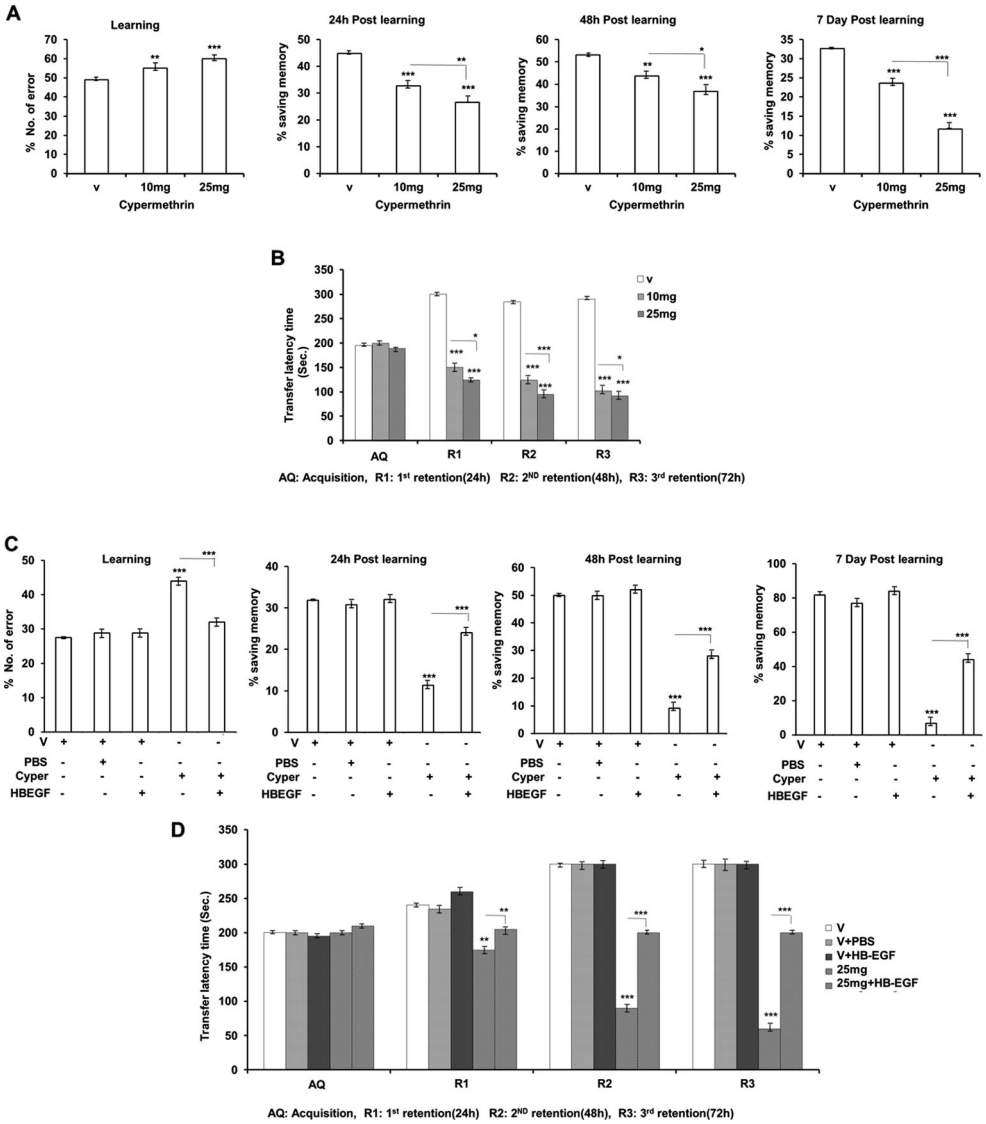

Fig. 6 Cypermethrin reduces learning-memory performance, which is prevented by exogenous HB-EGF. **a** Dose-dependent increase in the number of errors (%) during learning and fall in memory retained (% saving memory) at 24 h, 48 h, and 7 days post-learning in Y-Maze test. **b** Acquisition trial and dose-dependent fall in transfer latency time at first, second, and third retention trials in passive avoidance test. **c** Number of errors (%) during learning and memory retained (% saving memory) at 24 h, 48 h, and 7 days post-learning in Y-Maze test for rats treated with cypermethrin and/or HB-EGF. **d** Acquisition trial and transfer latency time at first, second, and third retention trials in passive avoidance test for rats treated with cypermethrin (25 mg/kg) and/or HB-EGF. Data represent means±SE of 20 rats. ***$P<0.001$, **$P<0.01$, and *$P<0.05$ compared to vehicle (V) or as indicated

and hippocampus. Activated astroglia stimulate the generation of IL-1 and overexpression of neuronal IL-1R1 (Suppl. 5A, showing the expression of IL-1R1 in neurons) that directly associates with neuronal Aβ and p-tau. An increase in the pro-amyloidogenic cleavage pathway of APP, characterized by enhanced APP, BACE activity, CTFβ, and PS results in elevated Aβ, and increase in tau and its GSK3β-mediated phosphorylation generates p-tau. Neuronal GSK3β (Suppl. 5B, showing the expression of GSK3β in neurons), via regulation of BACE activity, serves as the convergence point of amyloid and tau pathways, leading to increase in neuronal Aβ and p-tau. Eventually, the Aβ and p-tau accumulation in frontal cortex and hippocampus culminates in cognitive impairments in the young rats, which may be prevented by exogenous HB-EGF treatment (Fig. 7).

Discussion

Our data support the hypothesis that exposure to pesticides is an important risk factor for AD-like pathology. The findings are important because they reveal that cypermethrin evokes premature induction of neuronal Aβ and p-tau proteins, inducing cognitive impairments in young rats. The sequential event discerned is a reduction in HB-EGF signaling, which induces astroglial-NF-κB activation and neuroinflammation, resulting in GSK3β-dependent upregulation of amyloid and tau pathways in frontal cortex and hippocampus. Furthermore, our data reveal that a normal HB-EGF signaling prevents generation of the early manifestations of AD-like pathology (Fig. 7).

Early-life pesticide exposure is suggested playing a critical role in the onset of neurodegeneration at adulthood [42]. Supporting the concept, Parkinson's disease-like nigrostriatal

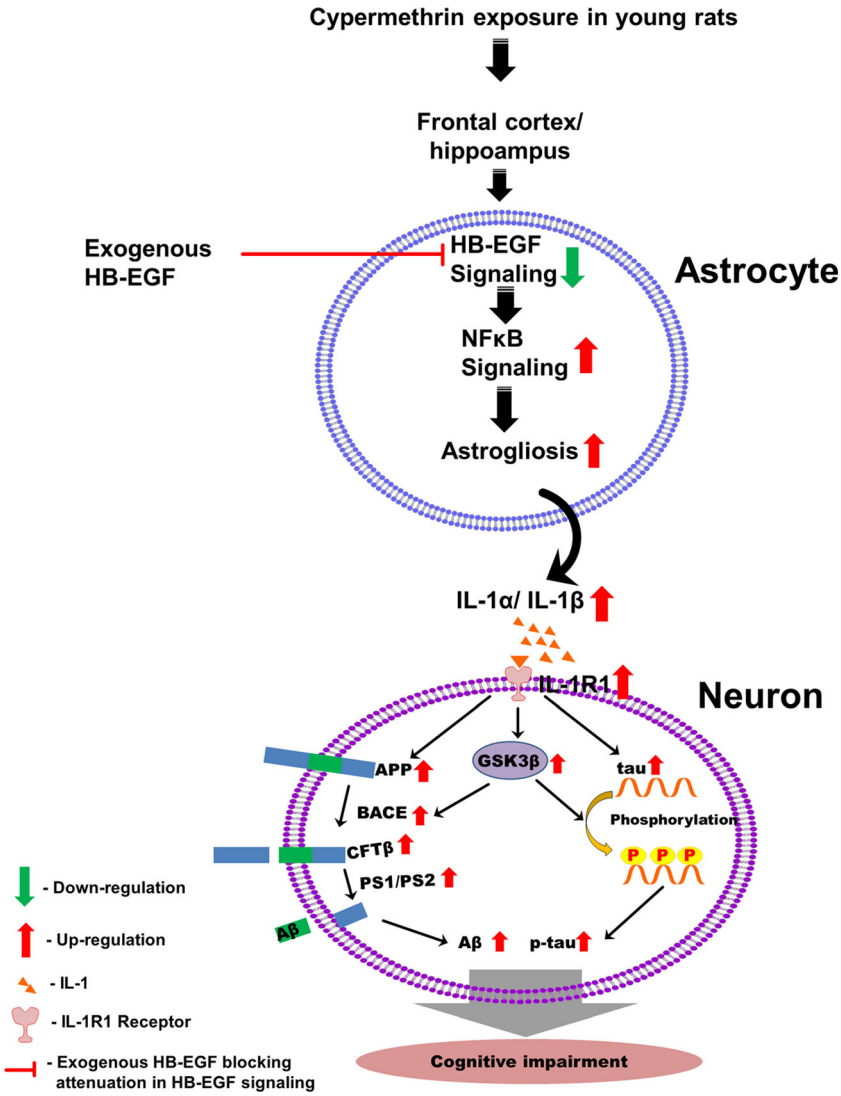

Fig. 7 Proposed schematic showing cypermethrin-induced early Aβ and p-tau induction, which is prevented by normal HB-EGF signaling. Cypermethrin downregulates HB-EGF signaling which upregulates astrocytic NF-κB signaling and enhances astrogliosis in rat frontal cortex and hippocampus. It further induces IL-1α and IL-1β and neuronal IL-1R1. Enhanced IL-1 stimulates induction of APP, tau, and GSK3β. APP undergoes amyloidogenic processing via a sequential increase in BACE activity, CTF-β, and PS1 and PS2 levels to generate Aβ. GSK3β causes phosphorylation of tau to generate p-tau and stimulates BACE activity to promote Aβ induction. Increased neuronal Aβ and p-tau in brain culminates in cognitive impairment. Exogenous HB-EGF blocks the attenuation in HB-EGF signaling and thereby prevents cypermethrin-mediated induction of Aβ and p-tau

dopaminergic neurodegeneration is observed in adult rats that have been exposed postnatally or re-challenged with cypermethrin during adulthood [5, 21]. However, the studies do not cite features of early-onset neurodegeneration upon developmental exposure to the pyrethroid. Here, our data demonstrate that cypermethrin elicits upregulation in both the major indicator protein molecules of AD, Aβ, and p-tau, even in adolescents (P-45), implying a strong neurodegenerative feature that appears to be independent of age. Though exposure to the pyrethroid, deltamethrin, is identified to induce tau hyperphorylation [43], to the best of knowledge, the effect of pyrethroids on the amyloid pathway is still unexplored. Our findings for the first time illustrate stimulation of both the major pathways of AD by a pyrethroid.

Our data reveal that cypermethrin stimulated a typical pro-amyloidogenic processing of APP through sequential activation of BACE and PS, elevating both the isoforms of Aβ. Nonetheless, a greater increase in $A\beta_{1–42}$ leading to an $A\beta_{1–42}/A\beta_{1–40}$ ratio >1.0 speculates increased stability of neuronal and synaptic toxic oligomers formed by the more aggregation prone $A\beta_{1–42}$ [36].

The current investigation uncovers that cypermethrin upregulates total tau and p-tau, suggestive of microtubule destabilization in the young rat brain [44]. Enhanced p-tau, with an ability to sequester normal tau and MAPs and deregulate tubulin assembling and axonal transport [45, 46], may account for cypermethrin-mediated neuronal dysfunctions. Consistent with earlier reports, the major tau kinase, GSK3β [47], played a key role in tau hyperphosphorylation. However, rather than its increased activity during aging [48], an augmented expression of GSK3β at an early-age facilitated premature neurodegeneration by cypermethrin.

Besides p-tau synthesis, GSK3β stimulated Aβ production as well, and therefore, appeared as a common molecular link between the two major pathways of AD-like pathology. Unlike earlier studies claiming a GSK3β-dependent direct modulation of PS [14, 15, 49], our finding demonstrates GSK3β-dependent BACE activation, i.e., a step prior to PS.

This is the second study after the one of Ly et al. [16] suggesting a direct link between BACE and GSK3β. An increase in NF-κB signaling by cypermethrin may justify this GSK3β-dependent activation of BACE, known to be regulated by NF-κB-p65-binding elements existing on BACE promoter [16].

The current investigation extends the results of our previous in vitro study in astrocytes [22], and demonstrates, in vivo, that cypermethrin inhibits HB-EGF-EGFR signaling in tissues of frontal cortex and hippocampus. Contrary to these observations, a direct association of Aβ toxicity with enhanced EGFR activation has been reported [50]. In addition, HB-EGF neutralizing antibody and pharmacological modulation of EGFR transactivation is identified abrogating neurodegeneration, including AD [26]. Conversely, it is also acknowledged that endogenous HB-EGF, via PI3K/AKT and MEK/ERK pathways [51, 52], promotes wound healing and tissue repair [53] and prevents seizure-induced neural injury [23]. Our earlier report that suggests contribution of astrocytic ERK1/2 and AKT activations, downstream of exogenous HB-EGF, in preventing cypermethrin-induced apoptosis [22] lends support to the HB-EGF-mediated protective viewpoint. However, it needs confirmation, whether these endogenous HB-EGF-activated MAPK and PI3K pathways participate in preventing AD.

While investigating the mechanism downstream of reduced HB-EGF, we identify an enhanced astrocytic NF-κB signaling and astrogliosis, which induced Aβ and p-tau in close vicinity of the astrocytes. HB-EGF, via blocking of NF-κB-activation, induces anti-inflammatory reaction in macrophages [54] and epithelial cells of the intestine [55, 56]. Nevertheless, there are no studies linking HB-EGF and NF-κB signaling in the brain. The current study, for the first time, demonstrates an inverse dependence of NF-κB signaling on HB-EGF in the astrocytes. As demonstrated earlier in intestinal epithelial cells [56], the cell-penetrating heparin-binding peptide domain from HB-EGF may be responsible for blocking phosphorylation of IκB and subsequent nuclear translocation of p65-NF-κB and thereby restricting NF-κB-dependent inflammatory responses in normal astrocytes. Cypermethrin, via suppression of HB-EGF, probably reduces penetration of the heparin-binding peptide domain in astrocytes, inducing neuroinflammation. Therefore, our findings help inferring that inhibition of astroglial NF-κB activation may represent one of the mechanisms by which HB-EGF exerts its anti-inflammatory and cytoprotective effects in the brain. Moreover, our previous report showing cypermethrin-mediated increase in intracellular astrocytic calcium and reactive oxygen species and upregulation in JNK and P38 signaling pathways [57], known to induce GFAP [58–60], substantiates astroglial activation detected here.

The current investigation reveals that cypermethrin stimulates the generation of IL-1, which causes induction of Aβ and p-tau. The data also demonstrate that Aβ and p-tau localized with IL-1R1, and akin to an earlier study on 3xTg-AD mice [61], IL-1Ra altered brain inflammatory responses and markedly alleviated GSK3β. Nevertheless, our data demonstrating IL-1Ra-mediated significant suppression of both p-tau and Aβ differs from that of the 3xTg-AD mice that demonstrates a considerable attenuation in tau pathology and partial reduction in Aβ by anti-IL-1R [61]. Our study emerges as one of the very few claiming direct dependence of both Aβ and p-tau on IL-1, as opposed to one claiming IL-1-mediated regulation of Aβ and tau pathology in opposing ways [20]. An IL-1-mediated enhancement in the precursor molecules, APP, and tau, as well as molecular link, GSK3β, by cypermethrin justifies regulation of IL-1-dependent Aβ and p-tau induction.

The mechanism responsible for IL-1-dependent increase in GSK-3β, APP, and tau is beyond the scope of this paper. However, dependence of GSK3β on IL-1 may be explained from our previous report showing a cypermethrin-mediated activation of p38-MAPK [57], known to mechanistically connect IL-1 with GSK-3β [61]. Upregulation of APP by IL-1 may be an outcome of enhanced APP translation via the APP-mRNA-5′ untranslated region that bears a functional IL-1 responsive element (IL-1RE) [19]. Regarding tau, to the best of knowledge, IL-1-mediated regulatory mechanism is absolutely unreported. Therefore, in the future, we aim at exploring specific mechanism of action of IL-1 on GSK3β, APP, and tau, upon cypermethrin exposure.

Going a step further in linking HB-EGF with neurodegeneration, our data demonstrate that cypermethrin generated learning and memory impairments, which could be prevented by exogenous HB-EGF. Synaptic dysfunction due to accumulation of Aβ and p-tau is well portrayed as one of the relevant reasons for cognitive degeneration in AD [62]. Secondly, HB-EGF is described to play an important role in synaptic plasticity and memory formation through regulation of the activity of $Ca^{(2+)}$/calmodulin-dependent protein kinases, glutamate receptor subunits, and nerve growth factors [24]. Therefore, disruption in HB-EGF signaling leading to neuronal accumulation of Aβ and p-tau may well explain cypermethrin-mediated cognitive degeneration and its protection by HB-EGF.

Conclusion

In summary, this study emphasizes the significance of cypermethrin in evoking early-age AD protein markers. It enlightens the biological mechanism that links a suppressed HB-EGF signaling to neuroinflammation and subsequent GSK3β-dependent Aβ and p-tau induction. Future studies are necessary to examine if the early-age AD-like pathology is irreversible or whether HB-EGF has the therapeutic potential of reversing the effects. In addition, understanding the

effect of cypermethrin on AD-like hallmarks in the elderly is needed.

Acknowledgments Funding from CSIR Network project-INDEPTH and miND are acknowledged. We acknowledge Dr. Debabrata Ghosh, CSIR-IITR, for helping in making Fig. 7; Mr Rajesh Khushwaha for helping in making Figs. 2 and 4; and Dr. Naibedya Chattopadhyay, CSIR-CDRI, for useful suggestions in writing the manuscript.

Conflict of Interest The authors declare no conflict of interest.

References

1. Maccioni RB, Munoz JP, Barbeito L (2001) The molecular bases of Alzheimer's disease and other neurodegenerative disorders. Arch Med Res 32:367–381
2. Parron T, Requena M, Hernandez AF, Alarcon R (2011) Association between environmental exposure to pesticides and neurodegenerative diseases. Toxicol Appl Pharmacol 256:379–385
3. Ray DE, Fry JR (2006) A reassessment of the neurotoxicity of pyrethroid insecticides. Pharmacol Ther 111:174–193
4. Gupta A, Agarwal R, Shukla GS (1999) Functional impairment of blood-brain barrier following pesticide exposure during early development in rats. Hum Exp Toxicol 18:174–179
5. Singh AK, Tiwari MN, Upadhyay G, Patel DK, Singh D, Prakash O et al (2012) Long term exposure to cypermethrin induces nigrostriatal dopaminergic neurodegeneration in adult rats: postnatal exposure enhances the susceptibility during adulthood. Neurobiol Aging 33: 404–415
6. Sery O, Povova J, Misek I, Pesak L, Janout V (2013) Molecular mechanisms of neuropathological changes in Alzheimer's disease: a review. Folia Neuropathol 51:1–9
7. Sobow T, Flirski M, Liberski PP (2004) Amyloid-beta and tau proteins as biochemical markers of Alzheimer's disease. Acta Neurobiol Exp 64:53–70
8. Fein JA, Sokolow S, Miller CA, Vinters HV, Yang F, Cole GM et al (2008) Co-localization of amyloid beta and tau pathology in Alzheimer's disease synaptosomes. Am J Pathol 172:1683–1692
9. Pozueta J, Lefort R, Shelanski ML (2013) Synaptic changes in Alzheimer's disease and its models. Neuroscience 251:51–65
10. Dodart JC, Mathis C, Ungerer A (2000) The beta-amyloid precursor protein and its derivatives: from biology to learning and memory processes. Rev Neurosci 11:75–93
11. Hardy J, Selkoe DJ (2002) The amyloid hypothesis of Alzheimer's disease: progress and problems on the road to therapeutics. Science 297:353–356
12. Pooler AM, Polydoro M, Wegmann S, Nicholls SB, Spires-Jones TL, Hyman BT (2013) Propagation of tau pathology in Alzheimer's disease: identification of novel therapeutic targets. Alzheimers Res Ther 5:49
13. Hooper C, Killick R, Lovestone S (2008) The GSK3 hypothesis of Alzheimer's disease. J Neurochem 104:1433–1439
14. Su Y, Ryder J, Li B, Wu X, Fox N, Solenberg P et al (2004) Lithium, a common drug for bipolar disorder treatment, regulates amyloid-beta precursor protein processing. Biochemistry 43:6899–6908
15. Qing H, He G, Ly PT, Fox CJ, Staufenbiel M, Cai F et al (2008) Valproic acid inhibits Abeta production, neuritic plaque formation, and behavioral deficits in Alzheimer's disease mouse models. J Exp Med 205:2781–2789
16. Ly PT, Wu Y, Zou H, Wang R, Zhou W, Kinoshita A et al (2013) Inhibition of GSK3beta-mediated BACE1 expression reduces Alzheimer-associated phenotypes. J Clin Invest 123:224–235
17. Griffin WS, Stanley LC, Ling C, White L, MacLeod V, Perrot LJ et al (1989) Brain interleukin 1 and S-100 immunoreactivity are elevated in Down syndrome and Alzheimer disease. Proc Natl Acad Sci U S A 86:7611–7615
18. Wang HM, Zhang T, Huang JK, Sun XJ (2013) 3-N-butylphthalide (NBP) attenuates the amyloid-beta-induced inflammatory responses in cultured astrocytes via the nuclear factor-kappaB signaling pathway. Cell Physiol Biochem 32:235–242
19. Rogers JT, Lahiri DK (2004) Metal and inflammatory targets for Alzheimer's disease. Curr Drug Targets 5:535–551
20. Ghosh S, Wu MD, Shaftel SS, Kyrkanides S, LaFerla FM, Olschowka JA et al (2013) Sustained interleukin-1beta overexpression exacerbates tau pathology despite reduced amyloid burden in an Alzheimer's mouse model. J Neurosci 33:5053–5064
21. Tiwari MN, Singh AK, Agrawal S, Gupta SP, Jyoti A, Shanker R et al (2012) Cypermethrin alters the expression profile of mRNAs in the adult rat striatum: a putative mechanism of postnatal pre-exposure followed by adulthood re-exposure-enhanced neurodegeneration. Neurotox Res 22:321–334
22. Maurya SK, Rai A, Rai NK, Deshpande S, Jain R, Mudiam MK et al (2012) Cypermethrin induces astrocyte apoptosis by the disruption of the autocrine/paracrine mode of epidermal growth factor receptor signaling. Toxicol Sci 125:473–487
23. Opanashuk LA, Mark RJ, Porter J, Damm D, Mattson MP, Seroogy KB (1999) Heparin-binding epidermal growth factor-like growth factor in hippocampus: modulation of expression by seizures and anti-excitotoxic action. J Neurosci 19:133–146
24. Oyagi A, Moriguchi S, Nitta A, Murata K, Oida Y, Tsuruma K et al (2011) Heparin-binding EGF-like growth factor is required for synaptic plasticity and memory formation. Brain Res 1419:97–104
25. Oyagi A, Hara H (2012) Essential roles of heparin-binding epidermal growth factor-like growth factor in the brain. CNS Neurosci Ther 18: 803–810
26. Martin R, Cordova C, Nieto ML (2012) Secreted phospholipase A2-IIA-induced a phenotype of activated microglia in BV-2 cells requires epidermal growth factor receptor transactivation and proHB-EGF shedding. J Neuroinflammation 9:154
27. Schenk GJ, Dijkstra S, van het Hof AJ, van der Pol SM, Drexhage JA, van der Valk P et al (2013) Roles for HB-EGF and CD9 in multiple sclerosis. Glia 61:1890–1905
28. Singh A, Yadav S, Srivastava V, Kumar R, Singh D, Sethumadhavan R et al (2013) Imprinting of cerebral and hepatic cytochrome p450s in rat offsprings exposed prenatally to low doses of cypermethrin. Mol Neurobiol 48:128–140
29. Tanno M, Kuno A, Ishikawa S, Miki T, Kouzu H, Yano T, et al. (2014) Translocation of GSK-3beta, a trigger of permeability transition, is kinase activity-dependent and mediated by interaction with VDAC2. J Biol Chem 289(42):29285–96
30. Phiel CJ, Wilson CA, Lee VM, Klein PS (2003) GSK-3alpha regulates production of Alzheimer's disease amyloid-beta peptides. Nature 423:435–439
31. Schmid AW, Lynch MA, Herron CE (2009) The effects of IL-1 receptor antagonist on beta amyloid mediated depression of LTP in the rat CA1 in vivo. Hippocampus 19:670–676
32. Sinha RA, Khare P, Rai A, Maurya SK, Pathak A, Mohan V et al (2009) Anti-apoptotic role of omega-3-fatty acids in developing brain: perinatal hypothyroid rat cerebellum as apoptotic model. Int J Dev Neurosci 27:377–383
33. Rai A, Maurya SK, Khare P, Srivastava A, Bandyopadhyay S (2010) Characterization of developmental neurotoxicity of As, Cd, and Pb mixture: synergistic action of metal mixture in glial and neuronal functions. Toxicol Sci 118:586–601
34. Engvall E, Perlmann P, Enzyme-linked immunosorbent assay (ELISA) (1971) Quantitative assay of immunoglobulin G. Immunochemistry 8:871–874

35. Yadav RS, Chandravanshi LP, Shukla RK, Sankhwar ML, Ansari RW, Shukla PK et al (2011) Neuroprotective efficacy of curcumin in arsenic induced cholinergic dysfunctions in rats. Neurotoxicology 32: 760–768
36. Kuperstein I, Broersen K, Benilova I, Rozenski J, Jonckheere W, Debulpaep M et al (2010) Neurotoxicity of Alzheimer's disease Abeta peptides is induced by small changes in the Abeta42 to Abeta40 ratio. EMBO J 29:3408–3420
37. Rodriguez JJ, Olabarria M, Chvatal A, Verkhratsky A (2009) Astroglia in dementia and Alzheimer's disease. Cell Death Differ 16:378–385
38. Akama KT, Albanese C, Pestell RG, Van Eldik LJ (1998) Amyloid beta-peptide stimulates nitric oxide production in astrocytes through an NFkappaB-dependent mechanism. Proc Natl Acad Sci U S A 95: 5795–5800
39. Yu AC, Lee YL, Eng LF (1991) Inhibition of GFAP synthesis by antisense RNA in astrocytes. J Neurosci Res 30:72–79
40. Eng LF, Ghirnikar RS, Lee YL (2000) Glial fibrillary acidic protein: GFAP-thirty-one years (1969-2000). Neurochem Res 25:1439–1451
41. Kamphuis W, Middeldorp J, Kooijman L, Sluijs JA, Kooi EJ, Moeton M et al (2014) Glial fibrillary acidic protein isoform expression in plaque related astrogliosis in Alzheimer's disease. Neurobiol Aging 35:492–510
42. Carloni M, Nasuti C, Fedeli D, Montani M, Amici A, Vadhana MS et al (2012) The impact of early life permethrin exposure on development of neurodegeneration in adulthood. Exp Gerontol 47:60–66
43. Chen NN, Luo DJ, Yao XQ, Yu C, Wang Y, Wang Q et al (2012) Pesticides induce spatial memory deficits with synaptic impairments and an imbalanced tau phosphorylation in rats. J Alzheimer's Dis 30: 585–594
44. Schraen-Maschke S, Sergeant N, Dhaenens CM, Bombois S, Deramecourt V, Caillet-Boudin ML et al (2008) Tau as a biomarker of neurodegenerative diseases. Biomark Med 2:363–384
45. Stoothoff WH, Johnson GV (2005) Tau phosphorylation: physiological and pathological consequences. Biochim Biophys Acta 1739: 280–297
46. Avila J, Lucas JJ, Perez M, Hernandez F (2004) Role of tau protein in both physiological and pathological conditions. Physiol Rev 84:361–384
47. Muyllaert D, Kremer A, Jaworski T, Borghgraef P, Devijver H, Croes S et al (2008) Glycogen synthase kinase-3beta, or a link between amyloid and tau pathology? Genes Brain Behav 7(Suppl 1):57–66
48. Wen Y, Planel E, Herman M, Figueroa HY, Wang L, Liu L et al (2008) Interplay between cyclin-dependent kinase 5 and glycogen synthase kinase 3 beta mediated by neuregulin signaling leads to differential effects on tau phosphorylation and amyloid precursor protein processing. Neuron 28:2624–2632
49. Takashima A, Murayama M, Murayama O, Kohno T, Honda T, Yasutake K et al (1998) Presenilin 1 associates with glycogen synthase kinase-3beta and its substrate tau. Proc Natl Acad Sci U S A 95: 9637–9641
50. Wang L, Chiang HC, Wu W, Liang B, Xie Z, Yao X et al (2012) Epidermal growth factor receptor is a preferred target for treating amyloid-beta-induced memory loss. Proc Natl Acad Sci U S A 109: 16743–16748
51. Jin K, Mao XO, Del Rio Guerra G, Jin L, Greenberg DA (2005) Heparin-binding epidermal growth factor-like growth factor stimulates cell proliferation in cerebral cortical cultures through phosphatidylinositol 3′-kinase and mitogen-activated protein kinase. J Neurosci Res 81:497–505
52. Jin K, Mao XO, Sun Y, Xie L, Jin L, Nishi E et al (2002) Heparin-binding epidermal growth factor-like growth factor: hypoxia-inducible expression in vitro and stimulation of neurogenesis in vitro and in vivo. J Neurosci 22:5365–5373
53. Marikovsky M, Breuing K, Liu PY, Eriksson E, Higashiyama S, Farber P et al (1993) Appearance of heparin-binding EGF-like growth factor in wound fluid as a response to injury. Proc Natl Acad Sci U S A 90:3889–3893
54. Lee JY, Seo YN, Park HJ, Park YJ, Chung CP (2012) The cell-penetrating peptide domain from human heparin-binding epidermal growth factor-like growth factor (HB-EGF) has anti-inflammatory activity in vitro and in vivo. Biochem Biophys Res Commun 419: 597–604
55. Mehta VB, Besner GE (2003) Inhibition of NF-kappa B activation and its target genes by heparin-binding epidermal growth factor-like growth factor. J Immunol 171:6014–6022
56. Mehta VB, Besner GE (2005) Heparin-binding epidermal growth factor-like growth factor inhibits cytokine-induced NF-kappa B activation and nitric oxide production via activation of the phosphatidylinositol 3-kinase pathway. J Immunol 175:1911–1918
57. Maurya SK, Mishra J, Tripathi VK, Sharma R, Siddiqui MH (2014) Cypermethrin induces astrocyte damage: role of aberrant Ca(2+), ROS, JNK, P38, matrix metalloproteinase 2 and migration related reelin protein. Pestic Biochem Physiol 111:51–59
58. Gonzalez A, Pariente JA, Salido GM (2007) Ethanol stimulates ROS generation by mitochondria through Ca2+ mobilization and increases GFAP content in rat hippocampal astrocytes. Brain Res 1178:28–37
59. Kleinman MT, Araujo JA, Nel A, Sioutas C, Campbell A, Cong PQ et al (2008) Inhaled ultrafine particulate matter affects CNS inflammatory processes and may act via MAP kinase signaling pathways. Toxicol Lett 178:127–130
60. Roy Choudhury G, Ryou MG, Poteet E, Wen Y, He R, Sun F et al (2014) Involvement of p38 MAPK in reactive astrogliosis induced by ischemic stroke. Brain Res 1551:45–58
61. Kitazawa M, Cheng D, Tsukamoto MR, Koike MA, Wes PD, Vasilevko V et al (2011) Blocking IL-1 signaling rescues cognition, attenuates tau pathology, and restores neuronal beta-catenin pathway function in an Alzheimer's disease model. J Immunol 187:6539–6549
62. Spires-Jones T, Knafo S (2012) Spines, plasticity, and cognition in Alzheimer's model mice. Neural Plast 2012:319836